CHAPTER III

LITERATURE REVIEWS

Toughness of PC/ABS blend depends on characteristics of the blend such as composition, rubber content in ABS, molecular weight of PC. Figure 3.1 reveals the curves of Charpy impact test reported for PC/ABS blend at various compositions. As seen in the figure, the samples with pure PC and 90 wt% of PC in the blend exhibit brittle behavior with a very fast fracture propagation mechanism. At the compositions between 90-50 wt% of PC in the blend, they exhibit a slowly ductile propagation mechanism of cracking. For the lower PC content, the fracture mechanism of the blend turns to brittle behavior until 20% of PC in the blend. After that, the fracture mechanism will change to semiductile behavior. The change of the fracture mechanism is better illustrated in Figure 3.2. The maximum impact stress and impact energy related to the curves of Figure 3.1 are reported as a function of alloy composition (Greco et al., 1994).

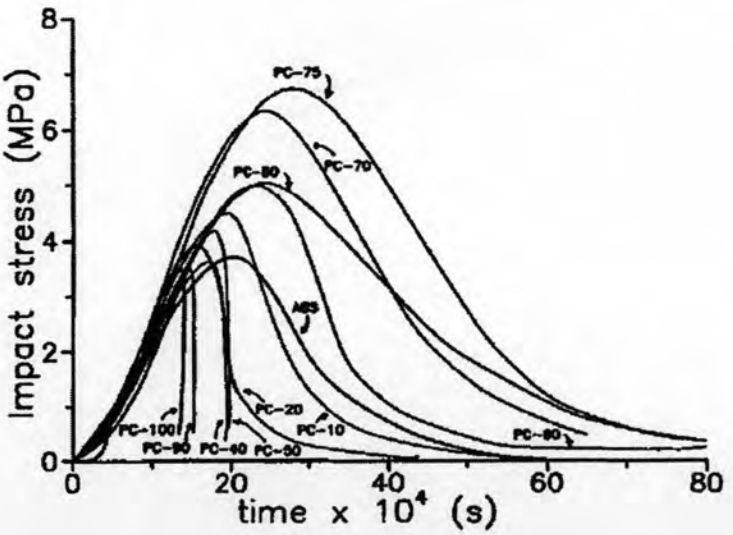

Figure 3.1 Curve of impact stress versus time of PC/ABS alloy at different PC composition (PC %) (Greco et al., 1994)

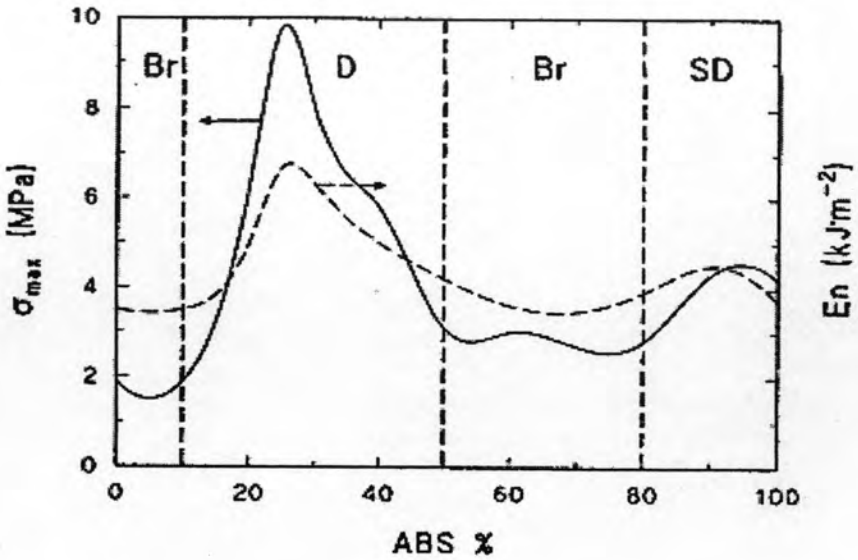

Figure 3.2 Maximum impact stress and energy for crack initiation versus ABS content. Br,brittle; D,ductile; SD,semiductile (Greco et al., 1994)

The superior fracture toughness of PC/ABS blend compared to that of pure PC and ABS results from enhanced energy absorption and inhibition or delay of crazing. Craze formation in PC matrix is an initiator of brittle failure.

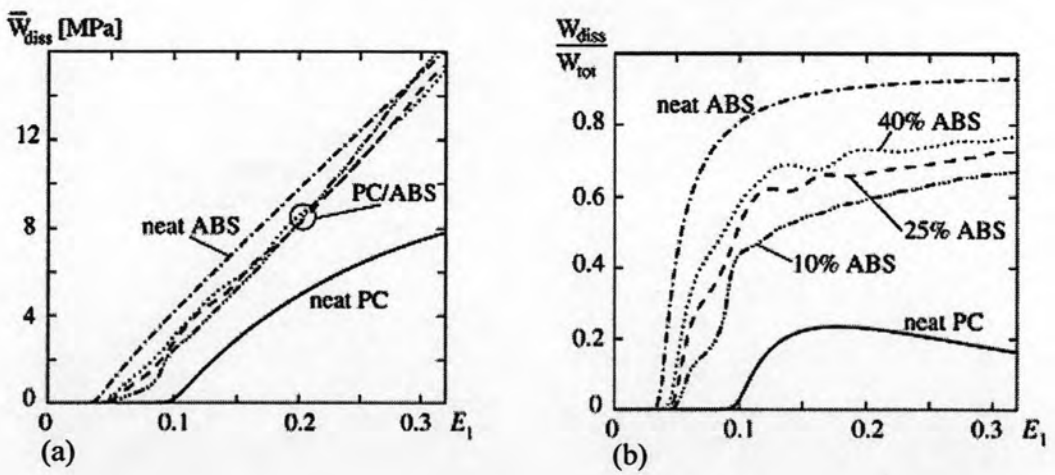

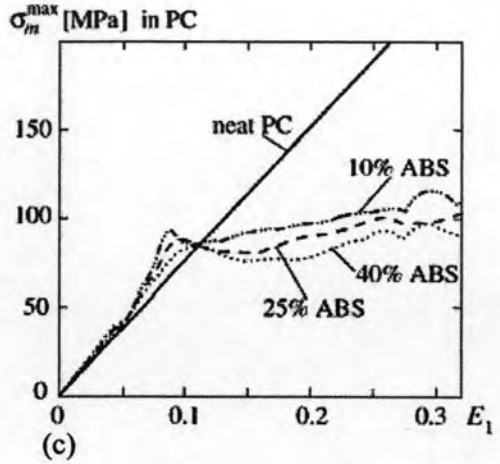

Figure 3.3 Effect of ABS volume fraction in blend: (a) work dissipated per volume of the blend, (b) dissipated work per total work, (c) peak values of hydrostatic stress in PC matrix (Seelig, Giessen, 2002)

For an ABS with 15 wt% rubber content, Figure 3.3(a) shows the absolute plastic dissipated work (W_{diss}) versus strain for PC/ABS with an ABS volume fraction of 0% (neat PC), 10%, 25%, 40% and 100% (neat ABS). From the figure, it can be seen that the absolute plastic dissipated work of all PC/ABS is higher than that of PC. Figure 3.3(b) reveals that W_{diss}/W_{tot}, i.e. the ratio of work dissipated in plastic deformation from total work applied, increases monotonically with the ABS content in the blend. The higher energy absorption in PC/ABS is due to contribution of yielding in ABS, which is the reason for the higher toughness. From the Figure 3.3(c), it reveals that the hydrostatic stress in neat PC increases linearly with strain. Whereas in PC/ABS blends, the peak values tend to be plateau about 100 MPa. This significant reduction of the peak of hydrostatic stresses in the neat PC matrix is due to volumetric expansion in ABS which enhances overall deformation (Seelig, Giessen, 2002).

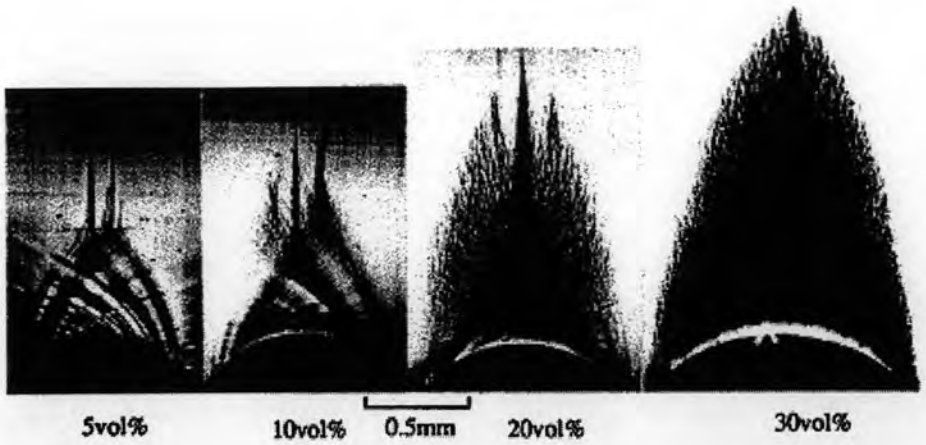

Figure 3.4 Local plastic zone of PC/ABS at various compositions (Ishikawa, 1995)

Figure 3.4 shows a local plastic zone of unbroken notched PC/ABS samples which were unloaded immediately before fracture in bending mode. At the low content of ABS, (5, 10 vol%), crazes initiated from the tip of notch will propagate to crack with low local plastic deformation region as shown in the figure. When the content of ABS is increased, the deformation mode is changed into a ductile mode which is shown by the higher plastic deformation region in the samples containing 20 and 30 vol% of ABS. It infers that the deformation mode of PC/ABS can be easily controlled by addition of small amount of the ABS (Ishikawa, 1995).

In this research, film stacking technique was used in our Kevlar-reinforced PC/ABS composite fabrication. The woven fibers and thermoplastic films were alternately stacked with a designed number of layers. After that, this stack was fused and pressed under high temperature and pressure. During the high pressure process, the molten thermoplastic was pushed trough the gap between the fibers and then the interface between the polymer matrix and fiber was formed. In this process, the high viscosity of the matrix influences difficulty of molten polymer to flow and wet into the fibers.

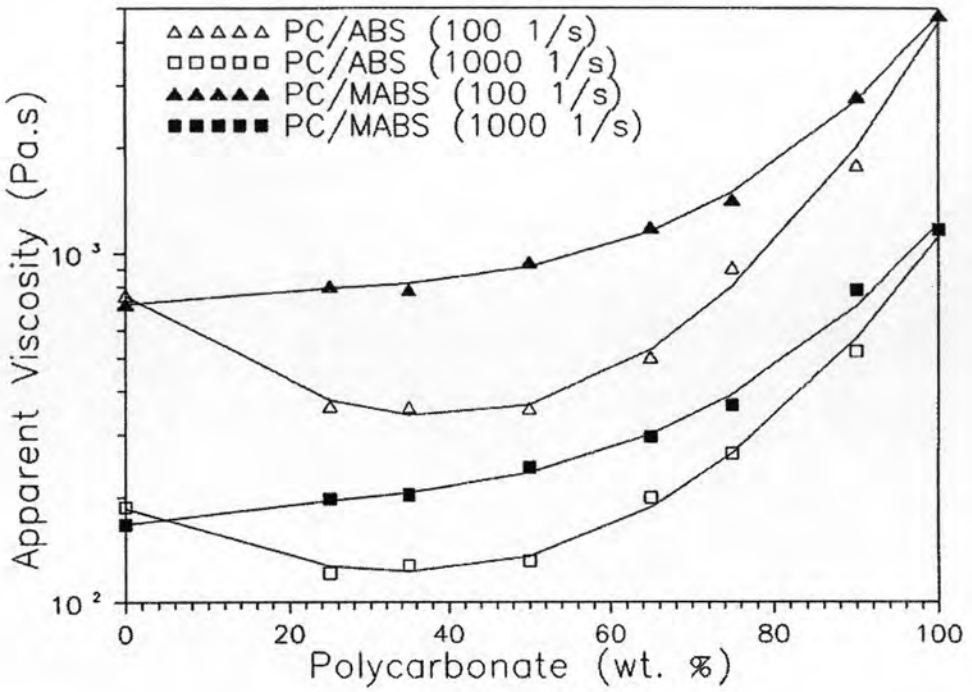

Figure 3.5 Apparent viscosity at shear rate 100 and 1000 s^{-1} versus blend composition for PC/ABS (Balakrishnan et.al., 1998)

Figure 3.5 depicts the viscosity of PC/ABS blends at various compositions. From the graph, it can be seen that the melt viscosities of PC/ABS blends are lower than that of ABS itself, up to 65wt% of PC in the blend. This low viscosity of PC/ABS blend may be because of three factors: (1) plasticisation; (2) degradation of PC by metal salts presenting in ABS; (3) poor interfacial interaction between the molten polymers. The plasticisation effect is caused by migration of low molecular weight species of PC and ABS. These species will migrate into another phase and reduce the interactive force between molecular chains in that phase, thereby allowing free movement of the chains. The metal salts presenting in ABS have been known to degrade PC in molten state, which produces low molecular weight fraction of PC. This fraction leads to the lower melt viscosity of the blend (Balakrishnan et.al., 1998).

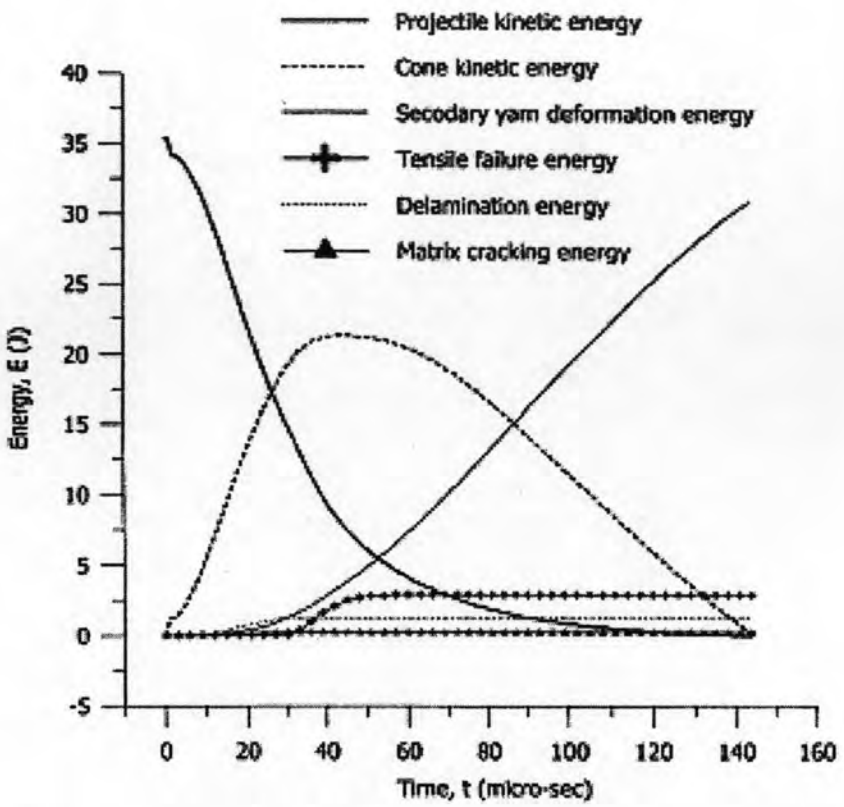

Figure 3.6 Energy absorbed by different mechanisms during ballistic impact of woven fabric E-glass/epoxy laminate (Naik et al., 2005)

Figure 3.6 shows energy of the projectile, which was absorbed by E-glass/epoxy composite with different energy absorption mechanisms. The impact velocity of a projectile used in this study was 158 m/s. In this case, the projectile kinetic energy was 34.9 J. At the end of the ballistic impact event, cone kinetic energy, secondary yarn deformation energy, tensile failure energy, delamination energy, and matrix cracking energy were 0.56%, 87.04%, 8.16%, 3.60% and 0.64% of total impact energy respectively. As a result of this research, the major portion of projectile kinetic energy was absorbed by the deformation of the secondary yarns. In addition, the energy absorbed by the deformation of the secondary yarns has two components, i.e. elastic strain energy and plastic deformation energy. If the projectile cannot complete penetrate to the target, elastic strain energy will be transferred back to the projectile, and the projectile will be rebounded (Naik et al., 2005).

For the best ballistic efficiency of a fiber reinforced composite, the polymer matrix content is preferred to be in the range of 20-25% by weight of the composite (Dickson et al., 1998; Park, 1996). The composite with low matrix content has high penetration resistibility but severe deformation after ballistic impact and it is not suitable for most applications. Moreover, the best mechanical properties are achieved at higher polymer matrix content but the ballistic efficiency will be decreased. To balance between mechanical and ballistic properties of our Kevlar-reinforced PC/ABS composites, the optimum fiber and matrix contents should be determined.

Morey et al. (2000) reported that the use of Kevlar fiber to produce ballistic composites with 50:50 mixture of phenol formaldehyde resin and polyvinyl butyral resin. The Kevlar composite of this resin mixture were 27 layers of Kevlar yielding 5.9 mm in thickness. It was capable to protect a projectile of 0.68 g steel sphere at 612 m/s strike velocity.

In the patent of Coppage et al. (2000), composite fabric comprised of aramid fiber combine with PBO fiber and at lest one flexible, rubbery resin used in making ballistic armor. The composite was able to pass the NIJ III-A (.44 magnum). The products possessed an areal density of 0.48 g/cm^2.

In the work of Pathomsap (2005), the composite comprised of at least 50 piles of the Kevlar cloth and 80:20 mixture of benzoxazine and urethane was reported to resist the ballistic impact at level III-A (9 mm). They also found that the 30-ply panel of the composite should be placed in the front face of the composite panel assembly to yield the best ballistic resistance. The products possessed an areal density of 0.24 g/cm^2 in the 10 piles/panel composites